Journal of Theoretical and Applied Information Technology
10th April 2016. Vol.86. No.1

ISSN: 1992-8645 www.jatit.org E-ISSN: 1817-3195

EDGE AND TEXTURE PRESERVING HYBRID ALGORITHM FOR DENOISING INFIELD ULTRASOUND MEDICAL IMAGES

P.V.V.KISHORE, D.KISHORE KUMAR, D.ANIL KUMAR, G.SAI PUJITHA, G.SIMARJEETH SINGH, K.BALA ANANTH SAI, K.MOHAN KALYAN,B.SRI SIVA ANANTA SAI,M.MANIKANTA,M.NANDA KISHORE

Department of Electronics and Communications Engineering, K.L.University, Guntur.

E-mail: pvvkishore@kluniversity.in, d.mohankishore@gmail.com, danilmurali@gmail.com, poojithagadireddy@gmail.com, simarjeethsingh@gmail.com,balukanugolu1995@gmail.com, mohankalyan2050@gmail.com, sivasai714@gmail.com, manikanta4460@gmail.com, nandakishore.m777@gmail.com

ABSTRACT

Medical Ultrasound Imaging is a rapidly growing allied field of Imaging Technology which is widely used around the world for diagnosis by clinicians. Non ionizing radiation is what makes ultrasound imaging safe for non-invasive imaging of human tissues. However, visual quality of ultrasound images poses a challenge for the medical practitioner due to multiple reflections of ultrasound signals. Numerous attempts have been made previously to improve the visual quality of the ultrasound images. The paper presents a novel, structured visual quality improvement mechanism based on daubechies (db) wavelet transform. In the proposed methodology, the segmentation of the ultrasound medical image is carried out with the help of active contour technique. The segmented image and the original image are transformed into wavelet domain. Selected wavelet coefficients are combined to improve the visual quality in terms of contrast and edges enhancements. Visual quality enhancement is emphasized with experimentation on medical ultrasound images obtained from AMMA Hospital radiology scanning center in India. Usefulness of the proposed algorithm is judged against denoising algorithms such as empirical mode decomposition (EMD), linear filtering (LF), median filtering (MF), wiener filtering (WF), wavelet based hard and soft thresholding and wavelet block based soft and hard thresholding. Visual quality metrics computed are peak signal to noise ratio (PSNR), normalized cross correlation (NCC), edge strength (ES), image quality index (IQI) and structured similarity index (SSI). Simulations demonstrate that the proposed enhancement algorithm outperformed the existing de-noising algorithms, instigating for actual medical application.

Keywords: *Ultrasound Medical Imaging, Active Contour, Discrete Wavelet Transform, Image Fusion, Image Denoising.*

1. INTRODUCTION

Ultrasound Imaging[1]-[3] has been in widespread use in medical analysis of late. This modality of medical imaging has become the most common imaging technique for diagnostic analysis due to the inherent feature of the noninvasiveness. Other advantages of Ultrasound imaging mechanism include low cost, portability and short time for generating images [4]-[6]. Research in this area has gained momentum in the recent past due to the fact that this imaging methodology is preferred by many a clinician/physician for diagnostic imaging though other high technology modalities such as Computed Tomography (CT) and Magnetic Resonance Imaging (MRI) are available. There is a growing interest among researchers to explore the usefulness of ultrasound imaging [7]-[9] in the low income countries as a commercially available premier diagnostics tool. In Ultrasound imaging the primary factor that is of concern is image quality [10]-[11]. The interpretation and analysis of ultrasound images is hampered seriously by the presence of dominant unwanted pixels called speckle. Numerous efforts are in place to augment these images for the purpose of getting legitimate and satisfactory information for diagnosis [12]-[14].

ISSN: 1992-8645 www.jatit.org E-ISSN: 1817-3195

In medical ultrasound imaging, a continual challenge that troubled many radiologists over the years is noise. Noise in ultrasound is integrated into the objects in the image making it difficult to obtain improved image quality for viewing [15]. De-noising is often an indispensable preprocessing step to be performed before exploiting the acquired data [16]. The existence of speckle [17] in medical ultrasound images makes the interpretation and diagnosis an uphill task. Thus a large set of de-speckling algorithms are proposed for analysis of ultrasound images.

Spatial filters [18] reduce the effects of image noise by smoothing, resulting in a major side effect called blur. Various new algorithms were proposed using the concepts of partial differential equations and computational fluid dynamics such as level set methods, total variation methods [19], nonlinear isotropic and anisotropic diffusion which claim to preserve the image edges. Mixed algorithms which combine impulse removal filters with local adaptive filtering in the transform domain to remove not only white and mixed noise, but also their mixtures [18] [14] are proposed. To reduce noise in ultrasound medical images algorithms involving digital filters (FIR or IIR), adaptive filtering (wiener filter), linear filtering, and median filtering are proposed in literature extensively and effectively [20]-[21]. Recent literature shows the use of wavelet domain for effectively de-noising medical images [22]-[23]. Soft and hard thresholding has successfully been applied by many researchers to reduce noise in wavelet domain. Recently empirical mode decomposition (EMD) [24] algorithm reported accomplishing de-noising of natural images based on Delaunay triangulation and on piecewise cubic polynomial interpolation.

This paper presents a different framework which exploits the inherent characteristic of Chen Vese (CV) active contour segmentation [25]-[26]. This is followed by implementation of de-noising the image in Discrete Wavelet Transform (DWT) [27] domain using a set of Daubechies wavelets (Harr, dbn and Sym) at 4 different levels of decomposition. Finally the image is subjected to 8 different image fusion rules which results in an enhanced output de-noised image. Parameter estimation of the proposed technique is carried out on the basis of five parameters that help in judging the quality of de-noised images from literature.

This paper is structured as follows. Section 2 presents a brief background of CV Active Contour technique based Segmentation along discrete wavelet transform based fusion algorithm for de-noising. Section 3 presents the proposed approach for ultrasound medical image enhancements. Section 4 presents the experimental observations and the results of the algorithm for verification. Finally, Section 5 concludes the paper with discussion.

2. BACKGROUND

2.1 Active Contours

Active contours are measurable curves that are used exclusively by image processing research community to extract object boundaries. Active contours come under a category of model based segmentation methods [28]-[30]. The fundamental design behind the active contours is the movement of a predefined contour within the domain of the image. Image domain is defined by the boundaries of objects in that particular image. Contour movement in the image domain is controlled by a parameter called energy function. The active contours model was first introduced by Terzopoulos [31]. Earlier models of active contours are prone to topological disturbances and are extremely susceptible to initial conditions. However with the development of level sets [26] topological changes in the objects of the image are involuntarily handled. Nevertheless all active contours depend on the gradient of the image for ending the growth of the curve.

2.2 Global Region Based Segmentation –The Chan Vese Model

Chan-Vese (CV) [26] active contour model discovers a contour $\Theta : D \rightarrow \Re^2$ defined on image space D consisting of a set of positive real numbers. The discovered contour optimally approximates the objects in a gray scale image $I^{xy} : D \rightarrow \Re^2$ to a single real gray value $\Phi^{(I)}$ on the inside of the contour Θ and another single gray level value $\Phi^{(E)}$ on the outside of the contour Θ. The basic idea of CV Active model is to find an optimal contour that fits the object boundaries. Alongside the best contour, the solution should also find a pair of optimal gray scale values $\Phi^F = \left(\Phi^{(I)}, \Phi^{(E)}\right)$ that discriminates object pixels from background pixels.

Mathematically the Chan-Vese active contour is formulated as an energy minimization problem

Journal of Theoretical and Applied Information Technology
10th April 2016. Vol.86. No.1

ISSN: 1992-8645 www.jatit.org E-ISSN: 1817-3195

$$E^{cv}\left(\Theta^F,\Phi^F\right)=\min_{\Phi} E^{cv}(\Theta,\Phi) \qquad (1)$$

Where, Θ^F is the final contour shape to be discovered and Θ is the initial contour chosen. The energy function or force function formulated by CV active contour model is minimized using piece wise linear Mumford-Shah [32] function which estimates the pixel values of a gray scale image I^{xy} by a linear piece wise smooth contour Θ.

The minimization problem is solved using the level set model [26] and is formulated in terms of level set function Θ^{xy} as

$$E^{cv}(\Theta,\Phi^{(I)},\Phi^{(E)})=\min_{\Theta,\Phi^{(I)},\Phi^{(E)}}\chi_2\left[\iint_{\mathrm{int}(\Theta)}(I^{xy}-\Phi^{(I)})^2\hbar\left(\Theta^{xy}\right)+\iint_{ext(\Theta)}(I^{xy}-\Phi^{(E)})^2(1-\hbar(\Theta^{xy}))dxdy\right]+\chi_1\int_{\Theta}\left|\nabla\hbar(\Theta^{xy})\right|dxdy \qquad (2)$$

where, $\hbar(\Theta)$ is Heaviside function. This minimization problem is solved by using Euler-Lagrange [26] equations and the level set function $\Theta(x,y)$ is updated iteratively by the gradient descent method as formulated below.

$$\Theta' = -\delta(\Theta)((I^{xy}-\Phi^{(I)})^2-(I^{xy}-\Phi^{(E)})^2-\chi_1\nabla.\frac{\nabla\Theta^{xy}}{\left|\nabla\Theta^{xy}\right|} \qquad (3)$$

Where x and y denote the locations of pixels in the image. $\delta(\Theta)$ is the delta function and $\Phi^{(I)}$ and $\Phi^{(E)}$ are updated iteratively using the equations

$$\Phi^{(I)}=\frac{\iint_{\Theta} I^{xy}\hbar(\Theta^{xy})dxdy}{\iint_{\Theta} H(\Theta^{xy})dxdy} \qquad (4)$$

$$\Phi^{(E)}=\frac{\iint_{\Theta} I^{xy}(1-H(\Theta^{xy}))dxdy}{\iint_{\Theta}(1-H(\Theta^{xy}))dxdy} \qquad (5)$$

The segmented ultrasound image contains the details of the object of interest (OOI) in a noisy image. We propose to fuse the ooi segments holding the edges of the original objects to improve the visual quality of ultrasound images.

2.3 DWT Based Fusion

CV active contour model provides as excellent framework for segmentation in ultrasound images under the influence of noise [26]. Though the segmentation using CV active contour is good, the visual quality is far from appealing to a normal human eye. Hence an attempt is being made in this paper to improve the visual quality of an ultrasound image by decreasing noise from the original image along with edge enhancement. For this purpose 2D discrete wavelet transform based fusion rules are used. In literature quite a number [33]-[34] of fusion rules are proposed by researchers. From them we attempt eight rules for our experimentation.

Image fusion processes blend two different sets of images by extracting information that is distinctive to a particular image, there by producing an improved image. Wavelet based medical image fusion has gained popularity in the recent past. In wavelet based fusion two images having unique properties are transformed using time frequency scaling of wavelet transform individually. Each image transformation produces four coefficients at assumed level 1, known as approximate coefficients and detailed coefficients. Different fusion rules on these transform coefficients such as max-min, max-max etc are applied. For example in min-min rule, minimum of approximate coefficients and minimum of detailed coefficients are preserved and 2D transformation model is created. Finally by applying 2D inverse transformation in wavelet domain fabricates into an enhanced fused image. Ten fusion rules namely {min-min, min-max, max-min, max-max, mean-mean, approx-scaling, approx-col- $co\tilde{l}$, differential thresholding, aus-mind, min-dus} are applied for de-noising and enhancing edges for improving the visual quality of medical ultrasound images. From the applied ten, two fusion rules stand out in providing quality images after reconstruction. Minimum -minimum fusion rule where approximate coefficients of original ultrasound are fused with minimum of details accordingly.

2D DWT of I_M^{xy} produces approximate coefficients $W_M{}^{\psi^A}$ and detailed coefficients $W_M{}^{\psi^H}, W_M{}^{\psi^V}$ and $W_M{}^{\psi^D}$. Similarly for CV segmented ultrasound image I_S^{xy} 2D DWT generates $W_S{}^{\psi^A}$ and detailed coefficients $W_S{}^{\psi^H}, W_S{}^{\psi^V}$ and $W_S{}^{\psi^D}$. The min-min fusion rule says select the minimum values from approximate coefficients and minimum values from detailed coefficients. Mathematically

Journal of Theoretical and Applied Information Technology
10th April 2016. Vol.86. No.1

ISSN: 1992-8645 www.jatit.org E-ISSN: 1817-3195

$$W_{\psi}^{F} = \begin{cases} \min(W_M{}^{\psi^A}, W_S{}^{\psi^A}) \\ \min(W_M{}^{\psi^H}, W_S{}^{\psi^H}) \\ \min(W_M{}^{\psi^V}, W_S{}^{\psi^V}) \\ \min(W_M{}^{\psi^D}, W_S{}^{\psi^D}) \end{cases} \quad (6)$$

Figure 1 explicates min-min fusion rule using multiresolution wavelet transform.

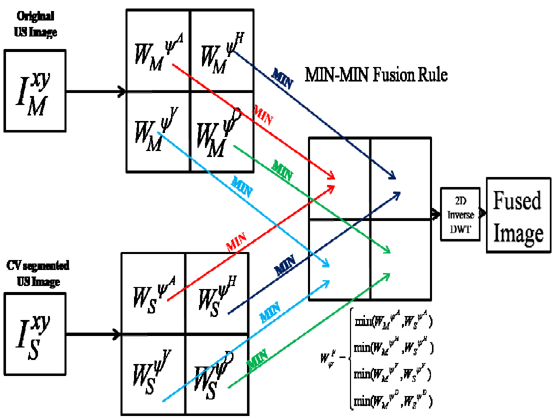

Figure.1. Min-Min Fusion Rule.

3. METHODOLOGY

To evaluate the proposed method, we use Chan Vese (CV) active contour model followed by DWT for multilevel medical image fusion. The general image fusion scheme using DWT is shown in Fig. 2.

The original Ultrasound Image is subjected to 2D DWT and the corresponding wavelet coefficients are obtained. The next step of the proposed technique is to apply the active contour on an ultrasound medical image to segment region of interest (ROI) sections of the image. Then the active contour segmented ultrasound image is also subjected to 2D DWT and the corresponding wavelet coefficients are obtained. The 2D DWT wavelet coefficients are computed for 8 different wavelets namely, Haar, db2, db4, db6, sym3, sym5, sym7and sym9 for 4 levels of decomposition. Once images are decomposed using DWT and wavelet coefficients are obtained, we have to select an appropriate fusion rule to combine wavelet coefficients of source images.

The 10 different fusion rules are formulated for carrying out the mixing of the original ultrasound and segmented ultrasound images. Inverse DWT is computed for the fused image for reconstructing the de-noised image. Improvement in quality is assessed by visually observing the images and their profiles before and after enhancement process. Quantitative measurements such as signal to mean square error (SSME), peak signal to noise ratio (PSNR), normalized cross correlation (NCC), image quality index (IQI) and structured similarity index (SSI) are computed between original and improved ultrasound images.

Experiments were conducted using 10 fusion rules with 8 different wavelets at 4 different levels. The best two fusion methods using a particular mother wavelet at a suitable level are presented here.

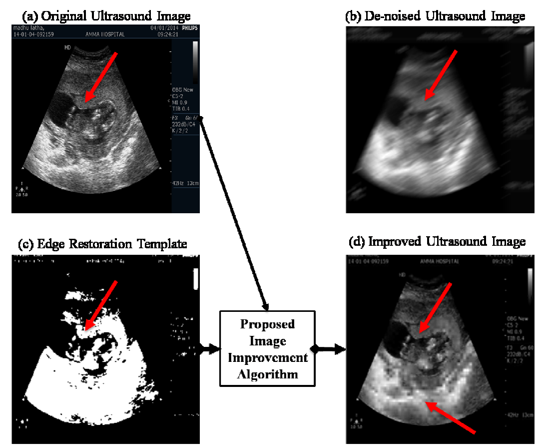

Figure.2. (a) *Original ultrasound image of a 10 week old fetus (b) de-noised image using linear filtering (c) active contour based segmented proposed algorithm using edge restore Ultrasound Medical Image.*

The proposed algorithm is applied on different ultrasound medical images converted to TIFF format. The step-wise sequence of the proposed mechanism is as follows:

Proposed Algorithm: Ultra Sound Medical Image De-noising

S1: Segment Ultrasound medical image using Chan Vese Active Contour model I_S^{xy} .

S2: Save the Segmented image in I_S^{xy} .

S3: Compute 2D discrete wavelet transform using fast filter bank approach on the original ultrasound medical image I_M^{xy} resulting in wavelet coefficients $W_M{}^{\psi^A}, W_M{}^{\psi^H}, W_M{}^{\psi^V}, W_M{}^{\psi^D}$

S4: Calculate fast 2D wavelet transform for active contour segmented ultrasound image I_S^{xy} followed by following wavelet coefficients $W_S{}^{\psi^A}, W_S{}^{\psi^H}, W_S{}^{\psi^V}, W_S{}^{\psi^D}$

S5: Use eight different mother wavelets to compute 2D DWT-{Haar, db2, db4,db6,sym3,sym5,sym7,sym9}.

Journal of Theoretical and Applied Information Technology
10th April 2016. Vol.86. No.1

ISSN: **1992-8645** www.jatit.org E-ISSN: **1817-3195**

S6: Formulate fusion rules to mix the wavelet coefficients to extract better coefficients from the two medical ultrasound images.

S7: Ten fusion rules formulated as {min-min, min-max, max-min, max-max, mean-mean, approx-scaling, approx-col-$co\tilde{l}$, aus-mind, min-dus and differential thresholding}.

S8: Compute 2D Inverse DWT to reconstruct the fused de-noised image.

S9: Calculate parameters to assess the strength of the output de-noised US medical image.

4. EXPERIMENTAL OBSERVATIONS AND RESULTS

Experiments are performed using different wavelets at various levels with multiple fusion rules. Experimental simulations for all the combinations of wavelets, their decomposition levels and fusion rules were conducted. Three types of images are chosen to perform the experiments which are obtained from radiology lab at AMMA Hospitals, Vijayawada. They are ultrasound images of fetus at various times of a pregnant woman obtained with Phillips sonographic machine at 42Hz, 13cm display as shown in Fig. 3(a)-(c).

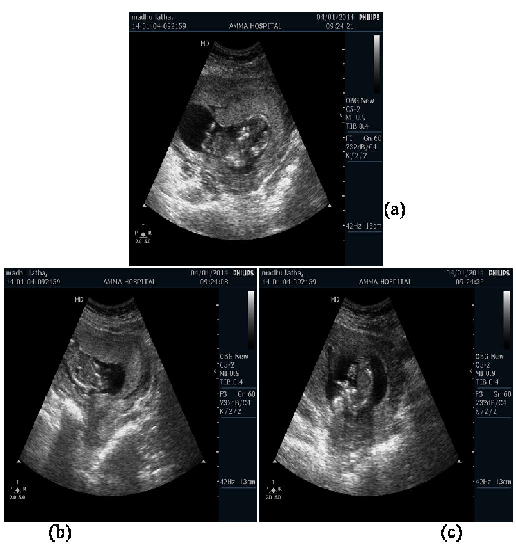

Figure.3. (A)-(C). Test Images Use For Experimentation From Phillips Sonographic Machine At AMMA Hospitals Radiology Lab At Vijayawada, India Of A Ten Week Old Pregnant

Each image is first resized to a standard resolution of 256×256 from their original resolutions. Eight different mother wavelets namely ‘haar’ or ‘db1’, ‘db2’, ‘db4’, ‘db6’, ‘sym3’, ‘sym5’, ‘sym7’, ‘sym9’ belonging to orthogonal family of daubechies(db) and symlets(sym) are tested. Four levels of decomposition are tested. Level-2 with db2 wavelet with min-min and approximate ultrasound image mixed with minimum details of its own segments provided the best results.

Chan-Vese (CV) active contour is an image object boundary based segmentation algorithm. It segments the ultrasound medical image to extract portions of the image that have edge boundaries. It is observed that segmentation by CV removes noise nicely but degrades information to maintain visual quality.

The CV active contour model applied to our test images Fig. 3(a) of a pregnant woman with superimposed contours of radius 9 mm and its corresponding segmentation of the ultrasound image is shown in Fig. 4.

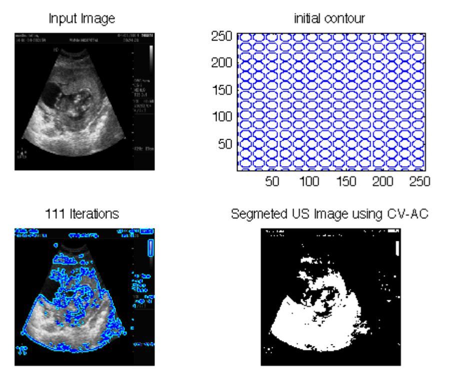

Figure. 4.Segmentation Of 10 Weeks Pregnant Woman Using CV Active Contour Model.

Final ultrasound segmented image reveals considerably fewer details visually but produces good object boundary. These boundaries play a vital role for the doctors to pin point the location of problems on the parts of the image. But when shown to doctors at the same hospital they were found to be uninterested in looking at the segmented image. Hence a model was proposed and developed to reduce speckle and improve the edge or boundary of the objects in the image. The speckle is reduced using multiresolution filter bank in wavelets and the boundary or edge strength of objects in the image is improved with fusion process.

Experimental simulations of the proposed algorithm were carried out on an Intel I3 machine with a 3GB RAM. Fig. 5 shows our proposed ultrasound medical image improvement algorithm output compared with regularly used de-noising algorithms for ultrasound image enhancement. The following algorithms are used for comparison:

Journal of Theoretical and Applied Information Technology
10th April 2016. Vol.86. No.1

ISSN: 1992-8645 www.jatit.org E-ISSN: 1817-3195

empirical mode decomposition (EMD), linear filtering (LF), median filtering (MF), wiener filtering (WF), wavelet based hard thresholding (WHT) and soft thresholding (WST) and wavelet block based soft(wbst) and hard thresholding(wbht). Fig. 5 shows response to the test ultrasound image in Fig. 3(a).

Observations from Fig. 5 clearly show the superiority of our proposed method with the rest of the enhancement algorithms. Comparing visually the improved images with Fig. 5(b), (c) and (d), the proposed algorithm outperforms in terms of image edge quality. Liner filter, median filter and wiener filter as shown in Fig. 5(b), (c) and (d) are implemented with a 3×3 window filter. Empirical mode decomposition (EMD) based denoising has superior denoising characteristics as proposed in [24]. EMD algorithm decomposes any input data using maxima and minima derived from the data itself. Then bspline interpolation is used to connect these values to create a string of oscillating components called intrinsic mode functions (IMF). Fig. 5(e) shows emd filtered ultrasound image with lost object information. Medical images have too many maxima and minima with sudden transitions resulting in deprived performance of EMD fitter. Soft and hard thresholding of wavelet coefficients did show significant improvements to the image. But the biggest drawback of thresholding methods is choosing the right threshold value. Hard thresholding is the simplest form of thresholding where the threshold value is chosen by the user. Hard thresholding is applied on the detailed coefficients using the formulation

$$D_m{}^L(i,j) = \begin{cases} D(i,j) & \text{if } |D(i,j)| > \xi \\ 0 & \text{if } |D(i,j)| \le \xi \end{cases} \quad (7)$$

Where $D_m(i,j)$ are the modified or thresholded coefficients at level L at location (i,j). Hard threshold $\xi^L = \frac{\max(\max(D^L)}{M}$.

Soft thresholding is computed on detailed coefficients of wavelet transformed ultrasound medical image using the following expression

$$D_m{}^L(i,j) = \begin{cases} \operatorname{sgn}\left(D^L(i,j) \times \left(\left|D^L(i,j)\right| - \xi\right)\right) & \text{if } |D(i,j)| > \xi \\ 0 & \text{if } |D(i,j)| \le \xi \end{cases} \quad (8)$$

Where sgn() is a signum function. Where $D_m(i,j)$ are the modified or thresholded coefficients at level L at location (i,j). ξ is the hard threshold value. Fig. 5(f) and (g) show soft and hard thresholding algorithms respectively. Each 3×3 block of detailed wavelet coefficients are modified using equations (7) and (8) resulting in a block based soft and hard thresholding algorithms as shown in Fig. 5(h) and (i).

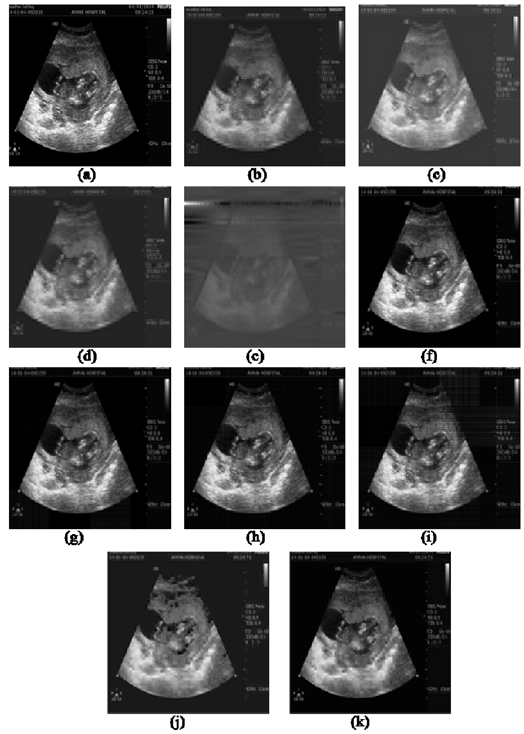

Figure.5. (a) Original ultrasound fetus images (b) Linear filter(LF),(c) median filter(MF), (d) wiener filter(WF) (e) EMD filter, (f) wavelet soft thresholding(WST), (g) wavelet hard thresholding(WHT), (h) Wavelet block soft thresholding (WBST), (i) wavelet block hard thresholding(WBHT) (j) Proposed active contour edge template with wavelet based min-min fusion, (k) proposed active contour edge template with wavelet based original ultrasound and minimum of wavelet details of template and original image.

Further testing is initiated on ultrasound images of Fig. 3(b) and 3(c). The responses of various algorithms along with the proposed method are recorded in Fig. 6 and Fig. 7 respectively.

Quantitative analysis with the help of image quality metrics is calculated using peak signal to noise ratio (PSNR), normalized cross correlation (NCC), edge strength(ES), image quality index (IQI) and structured similarity index (SSI) [35]-[37]. Table 1 formulates these values for the test ultrasound image in Fig. 3(a). The values in the last two rows indicate the robustness of the proposed method when compared to other commonly used algorithms.

Fig. 8 shows plot of PSNR (db) for various ultrasound image improvement algorithms. From the plot it becomes obvious that the proposed

Journal of Theoretical and Applied Information Technology
10th April 2016. Vol.86. No.1

ISSN: 1992-8645 www.jatit.org E-ISSN: 1817-3195

wavelet fusion methods show a remarkable improvement in the ultrasound image quality.

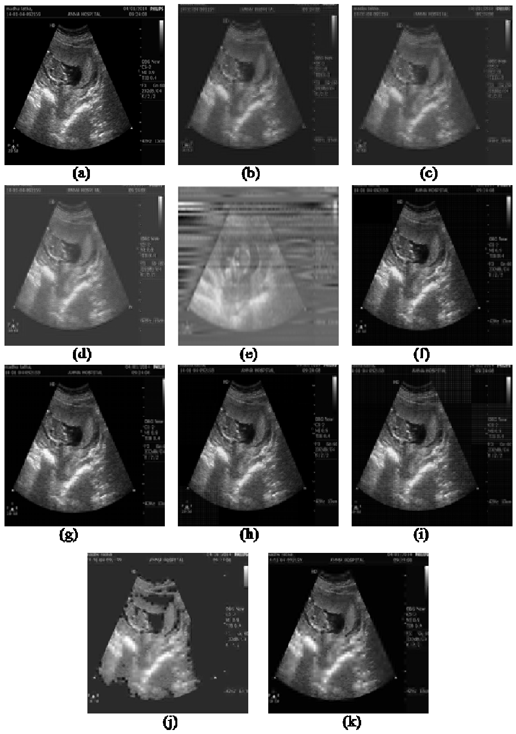

Figure. 6.(a) Original ultrasound fetus image from Fig. 3(b) (b) Linear filter(LF),(c) median filter(MF), (d) Wiener filter(WF) (e) EMD filter, (f) wavelet soft thresholding(WST), (g) wavelet hard thresholding (WHT) , (h) Wavelet block soft thresholding (WBST), (i) wavelet block hard thresholding(WBHT) (j) Proposed active contour edge template with wavelet based min-min fusion, (k) proposed active contour edge template with wavelet based original ultrasound and minimum of wavelet details of template and original image.

Table. I. Quality metrics for various ultrasound image improvement algorithms for image in Fig. 3(a).

Improvement Algorithm	PSNR(db)	NCC	ES	IQI	*SSI*
lf	22.580	0.796	0.646	0.631	0.657
mf	24.680	0.760	0.644	0.609	0.637
wf	25.900	0.810	0.677	0.632	0.648
emd	26.170	0.616	0.441	0.417	0.409
wst	24.190	0.838	0.689	0.711	0.672
wht	23.550	0.818	0.656	0.682	0.634
wbst	28.270	0.898	0.699	0.701	0.711
wbht	27.940	0.869	0.681	0.698	0.687
proposed(min-min fusion)	34.310	0.923	0.744	0.757	0.723
proposed(ous-min fusion)	36.890	0.953	0.782	0.772	0.758

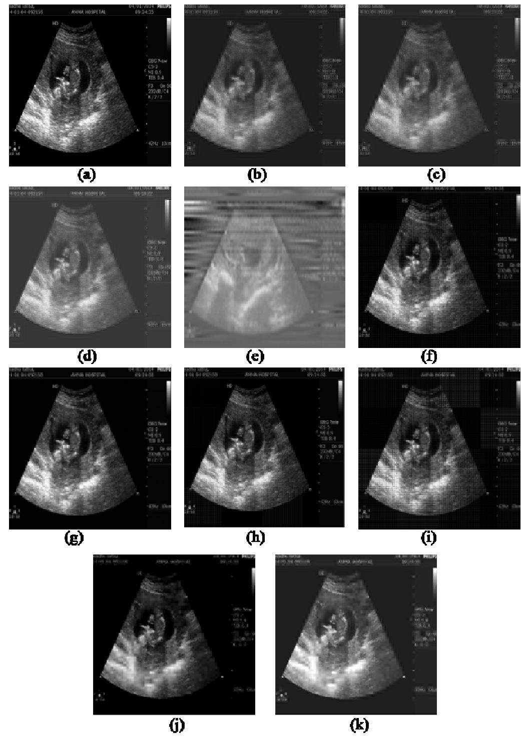

Figure. 7.(a) Original ultrasound fetus image from Fig. 3(c) (b) Linear filter(LF),(c) median filter(MF), (d) Wiener filter(WF) (e) EMD filter, (f) wavelet soft thresholding(WST), (g) wavelet hard thresholding (WHT), (h) wavelet block soft thresholding (WBST), (i) wavelet block hard thresholding(WBHT) (j) Proposed active contour edge template with wavelet based min-min fusion, (k) proposed active contour edge template with wavelet based original ultrasound and minimum of wavelet details of template and original image.

Fig. 9 indicates the remaining image quality metric values of various improvement algorithms against the proposed algorithm. These values are for ultrasound test image in Fig. 3(a). Values slightly differ for test images Fig. 3(b) and Fig. 3(c). PSNR for the proposed algorithm using min-min fusion rule is around 30db and for approximate original and details minimum is around 29db. These values indicate the novelty of the proposed method against the remaining algorithms. Similarly NCC is around 0.952 which is a good measure compared to other methods. Edge visibility in denoised ultrasound images is very weak. This edge strength measured for objects in the image is high for the proposed algorithms which are around 0.766. IQI and SSIM are two quality metrics proposed to measure the structured quality of the processed images. From the plot it can be observed these values are high compared to other algorithms. Max values of NCC, ES, IQI and SSIM are 1. Fig.

Journal of Theoretical and Applied Information Technology
10th April 2016. Vol.86. No.1

ISSN: 1992-8645 www.jatit.org E-ISSN: 1817-3195

10 compares PSNR (db) values for the three test images in Fig. 3. Little change can be observed in values from Fig. 3(c) from the previous two due a small change in contrast in the last image. But the PSNR values are within acceptable range for the proposed algorithm.

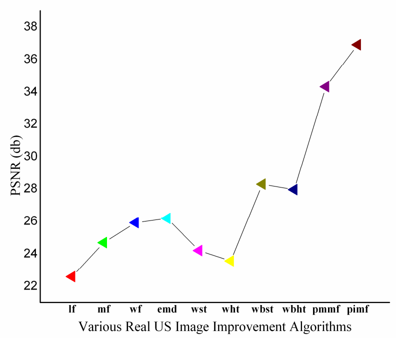

Figure.8. PSNR (db) plot for various ultrasound image improvement algorithms against the proposed algorithms.

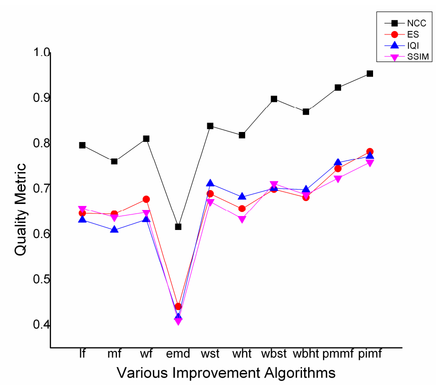

Figure.9.Various image quality metrics compared for ultrasound image improvement algorithms.

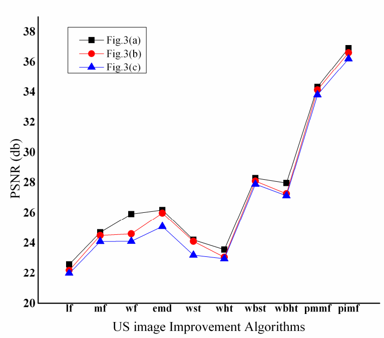

Figure.10. PSNR (db) computed for ultrasound test images in Fig.3 for various image improvement algorithms.

5. CONCLUSION

We have presented a technique for de-noising an ultrasound medical image and improve its visual features. Improvement in visual quality was accomplished using a novel wavelet based fusion algorithm which preserves boundary edges emulated from the active contour segmented ultrasound image. After experimentation with these methods it was found that min-min and aus-mind fusion rules suppress noise exceptionally well and retain edge features of the ultrasound objects in the image. Quality metrics computed suggest that the proposed algorithm has shown significant improvement to ultrasound image quality compared to previously proposed methods. Doctors at radiology department at AMMA Hospitals, Vijayawada were impressed by the results. By using the processed images their diagnostics time was reduced by 40%, which was measured with unprocessed and improved ultrasound images.

REFRENCES:

[1] G. Soloperto , F. Conversano , A. Greco , E. Casciaro , A. Ragusa , S. Leporatti , A. Lay-Ekuakille, S. Casciaro, "Multiparametric Evaluation of the Acoustic Behaviour of Halloysite Nanotubes for Medical Echographic Image Enhancement," *IEEE Transactions on Instrumentation & Measurement,* vol. 63, no.6, 2014, pp. 1423 – 1430.

[2] Lasso, A; Heffter, T., Rankin, A, Pinter, C. Ungi, T. Fichtinger, G., "PLUS:open-source toolkit for ultrasound-guided intervention systems", *IEEE Transactions on Biomedical Engineering*, vol.99, , 2014, pp.1-11.

[3] Chernyakova, T., Eldar, Y.C., "Fourier-domain beamforming: the path to compressed ultrasound imaging", *IEEE Transactions on Ultrasonics, Ferroelectrics and Frequency Control*, vol.61, no.8, 2014, pp.1252-1267.

[4] Tanter, M.; Fink, M., "Ultrafast imaging in biomedical ultrasound," *IEEE Transactions on Ultrasonics, Ferroelectrics, and Frequency Control,* , vol.61, no.1, 2014, pp.102-119.

[5] Conversano, F., Greco A., Casciaro, E., Ragusa, A., Lay-Ekuakille, A., Casciaro, S, "Harmonic Ultrasound Imaging of Nanosized Contrast Agents for Multimodal Molecular Diagnoses", *IEEE Transactions on Instrumentation & Measurement*, vol.61, no.7, 2014, pp.1848-1856.

ISSN: 1992-8645 www.jatit.org E-ISSN: 1817-3195

[6] Idzenga, T., Gaburov, E., Vermin, W., Menssen, J., De Korte, C., "Fast 2-D ultrasound strain imaging: the benefits of using a GPU", *IEEE Transactions on Ultrasonics, Ferroelectrics, and Frequency Control*, vol.61, no.1, 2014, pp.207-213.

[7] F. Conversano, E. Casciaro, R. Franchini, S. Casciaro, A. Lay-Ekuakille, "Fully Automatic 3D Segmentation Measurements of Human Liver Vessels from Contrast-Enhanced CT", *IEEE MeMea,* June, 11-12, 2014, Lisbon, Portugal.

[8] Rueda, S.; Fathima, S.; Knight, C.L.; Yaqub, M.; Papageorghiou, AT.; Rahmatullah, B.; Foi, A; Maggioni, M.; Pepe, A; Tohka, J.; Stebbing, R.V.; McManigle, J.E.; Ciurte, A; Bresson, X.; Cuadra, M.B.; Changming Sun; Ponomarev, G.V.; Gelfand, M.S.; Kazanov, M.D.; Ching-Wei Wang; Hsiang-Chou Chen; Chun-Wei Peng; Chu-Mei Hung; Noble, J.A, "Evaluation and Comparison of Current Fetal Ultrasound Image Segmentation Methods for Biometric Measurements: A Grand Challenge", *IEEE Transactions on Medical Imaging,* vol.33, no.4, 2014, pp.797-813.

[9] Yu-Hao Chen; Yu-Min Lin; Kuan-Yu Ho; An-Yeu Wu; Pai-Chi Li, "Low-Complexity Motion-Compensated Beamforming Algorithm and Architecture for Synthetic Transmit Aperture in Ultrasound Imaging", *IEEE Transactions on Signal Processing,* vol.62, no.4, 2014, pp.840-851.

[10] Fenster, A., Downey. D.B., "3-D ultrasound imaging: a review", *IEEE Engineering in Medicine and Biology Magazine*, vol.*15,* no.*6*, 2013, pp.41-51.

[11] Parker, K. J., M. M. Doyley, and D. J. Rubens. "Imaging the elastic properties of tissue: the 20 year perspective", *Physics in medicine and biology*, vol.56, no.1, 2011.

[12] C.P. Loizou, C.S. Pattichis, C.I. Christodoulou, "Comparative evaluation of despeckle filtering in ultrasound imaging of the carotid artery", *IEEE Transactions on Ultrasonics, Ferroelectrics and Frequency Control,* vol. 52,no.10, 2005, pp.1653–1669.

[13] Nima Torbati, Ahmad Ayatollahi, Ali Kermani, "An efficient neural network based method for medical image segmentation", *Computers in Biology and Medicine,* vol. 44, no. 1, 2014, pp.76-87.

[14] Loizou.C.P, Pattichis.C.S, Christodoulou.C.I, Istepanian.R.S.H, Pantziaris.M, Nicolaides.A, "Comparative evaluation of despeckle filtering in ultrasound imaging of the carotid artery", *IEEE Transactions on Ultrasonics, Ferroelectrics and Frequency Control*, vol.52, no.10, 2005, pp.1653-1669.

[15] Michailovich, O.V., Tannenbaum, A, "Despeckling of medical ultrasound images", *IEEE Transactions on Ultrasonics, Ferroelectrics, and Frequency Control*,vol.53, no.1, 2006, pp.64-78.

[16] Dantas, R.G., Costa, E.T., "Ultrasound speckle reduction using modified gabor filters", *IEEE Transactions on Ultrasonics, Ferroelectrics, and Frequency Control,* vol.54, no.3, 2007, pp.530-538.

[17] Juan L. Mateo, Antonio Fernández-Caballero, "Finding out general tendencies in speckle noise reduction in ultrasound images", *Expert Systems with Applications Elsevier,* vol.36, no. 4, 2009, pp.7786-7707.

[18] Munteanu, C., Morales, F.C., Ruiz-Alzola, J., "Speckle Reduction Through Interactive Evolution of a General Order Statistics Filter for Clinical Ultrasound Imaging", *IEEE Transactions on Biomedical Engineering,*vol.55, no.1, 2008, pp.365-369.

[19] Coupe, P., Hellier, P., Kervrann, C., Barillot, C., "Nonlocal Means-Based Speckle Filtering for Ultrasound Images", *IEEE Transactions on Image Processing,* vol.18, no.10, 2009, pp.2221-2229.

[20] Smital, L., Vítek, M., Kozumplík, J., Provazník, I, "Adaptive Wavelet Wiener Filtering of ECG Signals", *IEEE Transactions on Biomedical Engineering,* vol.60, no.2, 2013, pp.437-445.

[21] G. Andria, F. Attivissimo, G. Cavone, N. Giaquinto, A.M.L. Lanzolla, "Linear filtering of 2-D wavelet coefficients for denoising ultrasound medical images," *Measurement Elsevier,* vol. 45, no.7, 2012, pp.1792-1800.

[22] Gupta, N.; Swamy, M.N.S.; Plotkin, E., "Despeckling of medical ultrasound images using data and rate adaptive lossy compression", *IEEE Transactions on Medical Imaging,* vol.24, no.6, 2004, pp.743-754.

[23] Yong Yue; Croitoru, M.M.; Bidani, A; Zwischenberger, J.B.; Clark, John W., "Nonlinear multiscale wavelet diffusion for speckle suppression and edge enhancement in ultrasound images", *IEEE Transactions on Medical Imaging*, vol.25, no.3, 2006, pp.297-311.

[24] D. Labate, F. La Foresta, G. Occhiuto, F.C. Morabito, A. Lay-Ekuakille, P. Vergallo, "Empirical Mode Decomposition vs. Wavelet

ISSN: 1992-8645 www.jatit.org E-ISSN: 1817-3195

Decomposition for the extraction of respiratory signal from single-channel ECG: a comparison", *IEEE Sensors Journal*, vol.13, no.7, 2013, pp.2666-2674.

[25] Luminita Vese and Tony Chan, "A multiphase level set framework for image segmentation using the mumford and shah model," *International Journal of Computer Vision*, vol.*50*, no. *3*, 2002, pp.*271-293*.

[26] Chan.T, Vese.L.A, "Active contours without edges," *IEEE Transactions on Image Processing*, vol.10, no.2, 2001, pp.266–277.

[27] Aysal, T.C., Barner, K.E., "Rayleigh-Maximum-Likelihood Filtering for Speckle Reduction of Ultrasound Images", *IEEE Transactions on Medical Imaging*, vol.26, no.5, 2007, pp.712-727.

[28] M. Aventaggiato, F. Conversano, E. Casciaro, R. Franchini, A. Lay-Ekuakille, M. Muratore, S. Casciaro, "Automatic Segmentation of Vertebral Interfaces in Echographic Images," *3rd Imeko TC13 Symposium*, Lecce, Italy, April 17-18, 2014.

[29] Belaid, A., Boukerroui, D., Maingourd, Y., Lerallut, J-F, "Phase-Based Level Set Segmentation of Ultrasound Images", *Information Technology in Biomedicine, IEEE Transactions on* , vol.15, no.1, 2011, pp.138-147.

[30] Pereyra, M., Batatia, H., McLaughlin, S., "Exploiting Information Geometry to Improve the Convergence Properties of Variational Active Contours", *IEEE Journal of Selected Topics in Signal Processing,* vol.7, no.4, 2013, pp.700-707.

[31] M.Kass, A Witkin, D Terzopoulos ,"Snakes:active Contour Models", *International. Journal. of Computer Vision,*vol.1, pp. 321-331*,*1987.

[32] D. Mumford and J. Shah. "Optimal approximation by piecewise smooth functions and associated variational problems," *Comm. Pure Appl. Math,* vol.42, 1989, pp.577-*685*.

[33] Lifeng, Yu., Donglin, Zu., Weidong, Wang., Shanglian, Bao, "Multi-modality medical image fusion based on wavelet analysis and quality evaluation", *Journal of Systems Engineering and Electronics,* vol.12, no.1, 2001, pp.42-48.

[34] Yufeng Zheng, Edward A. Essock, Bruce C. Hansen, Andrew M. Haun, "A new metric based on extended spatial frequency and its application to DWT based fusion algorithms," *International Journal of Information Fusion,* vol. *8*, no.*2*, 2007, pp.177-192.

[35] A.M.L. Lanzolla, G. Cavone, M. Savino, M. Spadavecchia, "Analysis of influence parameters on image quality in ultrasound examination", *Proc. of MeMeA, Bari, Italy*, 2011, pp. 238–240.

[36] Z. Wang, A.C. Bovik, "A universal image quality index", *IEEE Signal Process. Lett*, vol.9, no.3, 2002, pp.81–84.

[37] Z. Wang, A.C. Bovik, H.R. Sheikh, E.P. Simoncelli, "Image quality assessment: from error visibility to structural similarity", *IEEE Trans. Image Process,* Vol.13, no.4, 2004, pp.600–612.